Highly Integrated Millimeter-Wave Passive Components Using 3-D LTCC System-on-Package (SOP) Technology

Jong-Hoon Lee, *Student Member, IEEE*, Gerald DeJean, *Student Member, IEEE*, Saikat Sarkar, *Student Member, IEEE*, Stephane Pinel, *Member, IEEE*, Kyutae Lim, *Member, IEEE*, John Papapolymerou, *Senior Member, IEEE*, Joy Laskar, *Senior Member, IEEE*, and Manos M. Tentzeris, *Senior Member, IEEE*

***Abstract* – In this paper, we demonstrate the development of advanced 3-D low-temperature cofired ceramic (LTCC) system-on-package (SOP) passive components for compact, low cost millimeter-wave wireless front-end modules. Numerous miniaturized easy-to-design passive circuits that can be used as critical building blocks for millimetre-wave SOP modules have been hereby realized with high performance and high integration potential. One miniaturized slotted patch resonator has been designed by the optimal use of vertical coupling mechanism and transverse cuts and has been utilized to realize compact duplexers (39.8 GHz/59 GHz) and 3 and 5 poles band pass filters by the novel 3D (vertical and parallel) deployment of single-mode patch resonators. Measured results agree very well with the simulated data. Also, one multiplexing filter, called directional channel-separation filter, that can be used in mixer applications shows insertion loss of <3dB over the bandpass frequency band and a rejection ~ 25dB at around 38.5GHz over the band rejection section. LTCC fabrication limitations have been overcome by using vertical coupling mechanisms to satisfy millimetre-wave design requirements. Last, a double fed cross-shaped microstrip antenna has been designed for the purpose of doubling the data throughput by means of a dual-polarized wireless channel, covering the band between 59-64 GHz. This antenna can be easily integrated into a wireless millimeter-wave link system.**

***Index Terms* – patch resonator, duplexer, low-temperature co-fired ceramic (LTCC), system-on-package (SOP), directional filter, multiplexing, 3D/vertical integration, microstrip antenna, dual polarization, millimeter-wave (mmW)**

I. Introduction

EMERGING millimeter-wave electronics for commercial applications, such as short-range broadband wireless communications, automotive collision avoidance radars and local cellular radio network (LCRN) require low manufacturing cost, excellent performance, and high level of integration [1]. The recent development of the multilayer low-temperature cofired ceramic (LTCC) System-On-Package (SOP) [2] makes these requirements achievable, because it offers a great potential for passives integration and enables microwave devices to be fabricated with high reliability, while maintaining a relatively low cost . Numerous publications [2] – [10] have dealt with the development of 3-D LTCC passive components that are critical building blocks in multilayer high-density architectures. However, recently reported structures do not use any miniaturization mechanism to be efficiently integrated as a building block into compact mmW/V-band SOP modules.

In this paper, we present the development of various advanced 3-D LTCC SOP passive building blocks enabling a complete passive solution for compact, low cost wireless front-end modules to be used in millimetre-wave frequency ranges. In order to realize compact and highly integrated bandpass filters, the performance of single-mode slotted patch resonators is first investigated at two operating frequencies (59.3GHz, 38.6GHz). After ensuring their excellent performance based on simulated and experimental results , one compact multilayer duplexer, which uses a via junction as a common input, has been realized to cover two bands (39.8 GHz/ 59GHz) for dual band mobile communication systems, such as wireless radio local area networks or local cellular radio networks (LCRN) [15]. In order to achieve a high out-of-band rejection a novel compact geometry of 3- and 5- poles bandpass filters has been implemented by cascading single mode-patch resonators on different layers with optimized inter-resonator coupling separation. A 4-port directional filter using embedded microstrip lines operating at 40GHz is also demonstrated and provides an easy and compact solution for mm-wave hybrid passive mixers. In the last section, a cross-shaped antenna has been designed for a dual-polarized transmission and reception of signals that cover the band between 59-64 GHz, in a configuration that can be easily integrated into wireless millimeter-wave transmit/receive modules.

All fabricated filters and antennas were measured using the Agilent 8510C Network Analyzer, Cascade Microtech probe station with 250 μm pitch air coplanar probes and a standard SOLT calibration method.

II. Patch Resonator Band Pass Filter (BPF)

A. Single Resonator Filter

Integrating filter on-package in LTCC multilayer technology is a very attractive option for RF front-ends up to mm-wave frequency range in terms of both

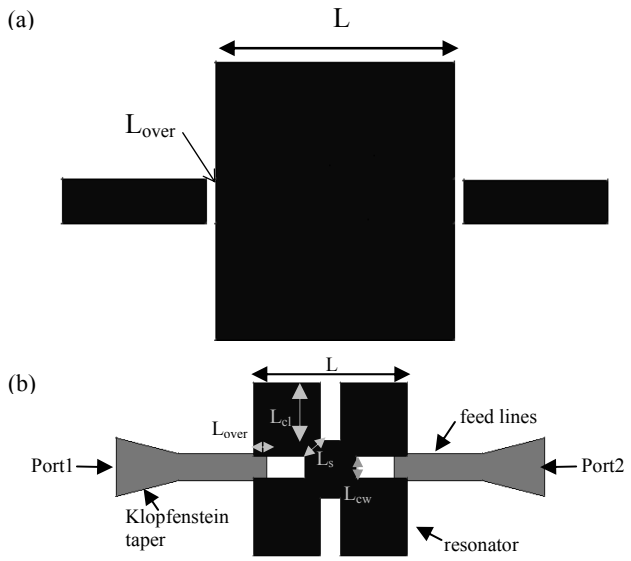

Fig. 1 Top view of (a) basic λ/2 square patch (b) Miniaturized patch resonator

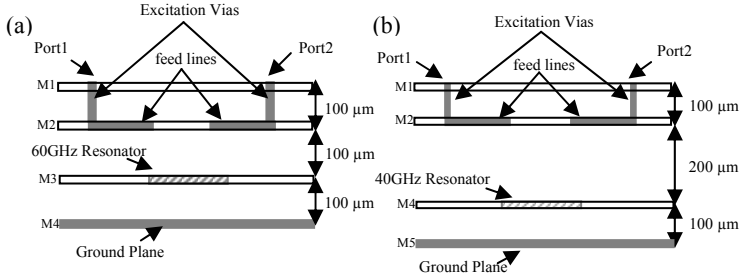

Fig. 2 Side view of multilayer configuration of (a) 60GHz slotted patch resonator (b) 39 GHz slotted patch resonator

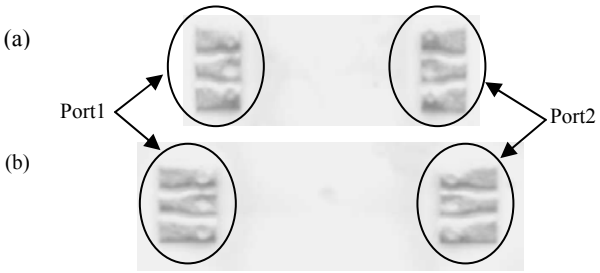

Fig. 3 The photographs of fabricated filters with coplanar waveguide (CPW) pads (a) at 60GHz (b) at 39 GHz

miniaturization by vertical deployment of filter elements and reduction of the number of components and assembly cost by eliminating the demand for discrete filters. In mm-wave frequencies the band pass filters are commonly realized using slotted patch resonators due to their miniaturized size, their excellent compromise between size, power handling and easy-to-design layout [3]. In this section, the design of a single-pole slotted patch filter is presented for two operating frequency bands (38-40 GHz and 58-60GHz). All designs have been simulated using the MOM-based, 2.5D full-wave solver IE3D.

Fig. 1 shows a top-view comparison between basic half-wavelength square patch resonator (L × L = 0.996 mm × 0.996 mm)[21] (fig. 1 a)) and the new configuration

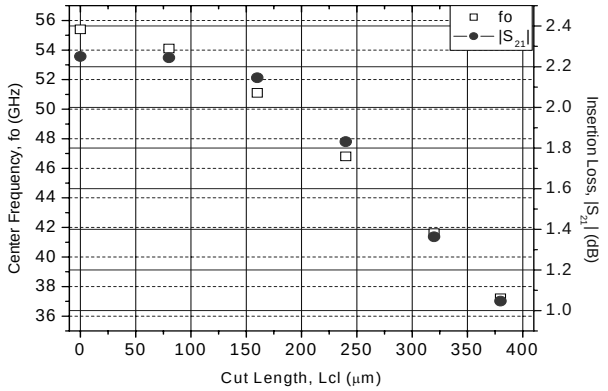

Fig. 4 Simulated responses of center frequency (f_o) and insertion loss ($|S_{21}|$) as a function of transverse cut (L_{cl})

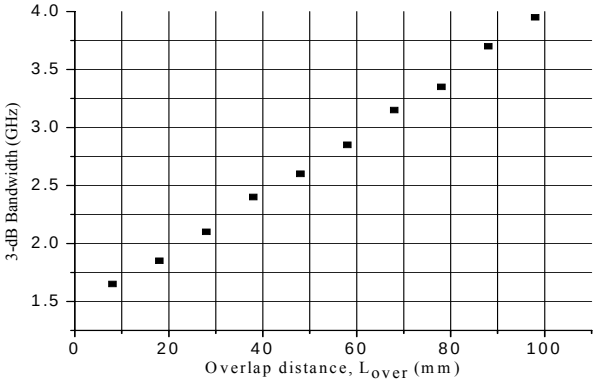

Fig. 5 Simulated 3-dB bandwidth as function of Overlap distance of (a) 60 GHz slotted patch resonator (b) 39 GHz slotted patch resonator

(L×L=0.616mm×0.616mm) capable to provide good tradeoffs between miniaturization and power handling (fig. 1b)). Side view and the photograph of the resonators for two operating frequency bands are shown in fig.2 and fig.3, respectively. In the design of λ/2 square patch, the planar single-mode patch and microstrip feedlines are located at metal 3 (M3 in fig. 2 a)) and use the end-gap capacitive coupling between the feedlines and the resonator itself in order to achieve 3 % 3dB bandwidth and <3dB insertion loss around the center frequency of 60 GHz. However, the required coupling capacitances to obtain design specifications could not be achieved because of the LTCC design rules limitations. In order to maximize the coupling strength, while minimizing the effects of the fabrication, the proposed novel structure takes advantage of the vertical deployment of filter elements by placing the feed lines and the resonator into different vertical metal layers as shown as fig. 2 a). This transition also introduces a 7.6% frequency downshift because of the additional capacitive coupling effect as compared to the basic λ/2 square patch resonator (fig. 1 a)) directly attached by feedlines.

Transverse cuts have been added on each side of the patch in order to achieve significant miniaturization of the patch by adding additional inductance. Fig 4 shows the simulated response for the center frequency and the insertion loss as the length of cuts (L_{cl} in fig. 1 b)) increases

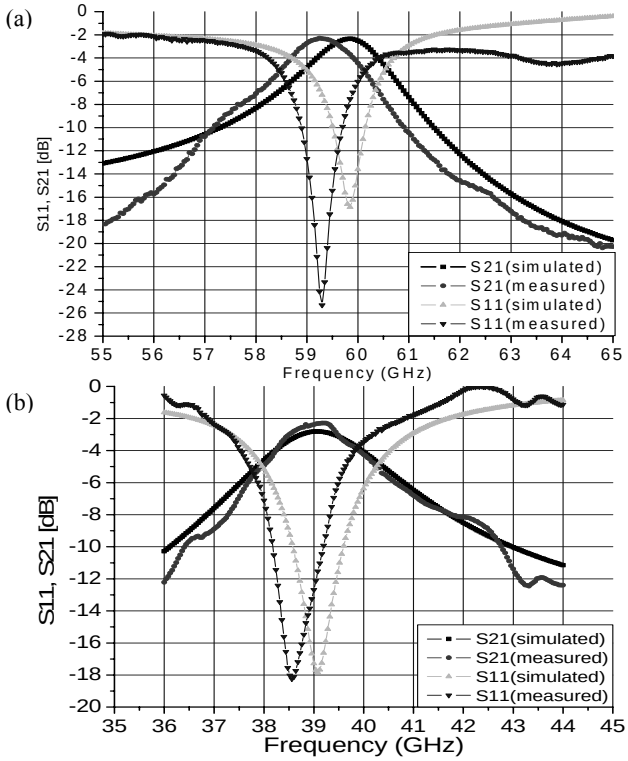

Fig. 6 Measured and simulated S-parameters of (a) 60 GHz slotted patch resonator (b) 39 GHz slotted patch resonator

while the fixed width of cuts (L_{cw}=L/8 in fig. 1 b)) is determined by the fabrication tolerance. It can be observed that the operating frequency range shifts further downward about 33% as the length of cut (L_{cl} in fig. 1 b)) increases by approximately 379 μm. Additional miniaturization is limited by the minimum distance (Ls in fig. 1 b)) between the corners of adjacent orthogonal cuts. Meanwhile, as the operating frequency decreases, the shunt conductance in the equivalent circuit of the single patch also decreases because its value is reciprocal to the exponential function of the operating frequency [16]. This fact additionally causes the reduction of radiation loss since it is proportionally related to the conductance in the absence of conductor loss [17]. Therefore, insertion loss at resonance is improved from 2.27 dB to 1.06 dB by an increase of L_{cl} in fig. 1 b).

The patch size is reduced significantly from 0.996 mm to 0.616 mm. The modification of bandwidth due to the patch's miniaturization can be compensated by adjusting the overlap distance (L_{over}). Fig.5 shows the simulated response for 3-dB bandwidth as L_{over} increases. It is observed that 3-dB bandwidth increases as L_{over} increases due to a stronger coupling effect and then L_{over} is determined to be 18 μm corresponding to 1.85 GHz 3-dB bandwidth.

The proposed embedded microstrip line filters are excited through vias connecting the coplanar waveguide signal pads on the top metal layer (M1 in fig. 2a)), reducing radiation loss compared to microstrip lines on the top (surface) layer. As shown in fig. 1 b), Klopfenstein impedance tapers are used to connect the 50Ω feeding line and the via pad on the metal 2 (M2 in fig. 1 b)). The overlap (L_{over}≈L/31) and transverse cuts (L_{cw}≈L/8, L_{cl}≈L/3.26) have been finally determined to achieve desired filter characteristics with aid of IE3D. Fig 3 a) shows the photograph of the fabricated filter prototypes with coplanar waveguide (CPW) pads fabricated in LTCC (ε_r=5.4, tanδ=0.0015) with a dielectric layer thickness of 100 μm and metal thickness of 9 μm. The overall size is 4.018 mm × 1.140 mm × 0.3 mm including the CPW measurement pads. As shown in fig. 6 a), the experimental and the simulated results agree very well. It can be easily observed that the insertion loss is < 2.3 dB, the return loss >25.3 dB over the pass band and the 3dB bandwidth is about 1 GHz. The center frequency shift from 59.85 GHz to 59.3 GHz can be attributed to the fabrication accuracy (vertical coupling overlap affected by the alignment between layers, layer thickness tolerance). This was the first fabrication iteration and the differences could be corrected in the second and third iterations.

The proposed slotted-patch filter architecture was also used in the design of mobile satellite communication systems around 39 GHz. The 39GHz single-mode patch filter (L×L =1.021mm×1.021 mm) was designed for 3.08% bandwidth, 39 GHz center frequency, and <3dB insertion loss. The design procedure was similar to the 60GHz filter except from the fact that the resonator was placed on two layers (instead of one layer) beneath the feeding lines as shown in the side view of fig. 2 b). The overlap (L_{over}≈L/7) and the transverse cuts (L_{cw}≈L/8.2, L_{cl}≈L/3) were determined to achieve the desired filter characteristics. The overall size was 4.423 mm × 1.140 mm× 0.4 mm with CPW measurement pads. The fabricated filter (fig. 3 b)) exhibits a minimum insertion loss of 2.3 dB, a return loss of 18.2 dB, and a 3-dB bandwidth about 3%. (fig. 6 b)) The experimental error in the calculation of the center frequency can be attributed to the fabrication accuracy as mentioned in 60GHz case.

B. DUPLEXER (41GHZ/61GHZ)

Recently, X band H-plane ridge waveguide duplexer was built in LTCC and experimentally succeeded [9]. Also, GSM (f_o = 0.92 GHz)/DCS (f_o = 1.77GHz) duplexer was implemented to be integrated into LTCC switch/filter front-ends module with excellent performance such as 0.5/0.9 dB insertion loss and 26.7 dB/ 27.9 dB. return loss [10]. However, to the best knowledge of authors, no duplexers of compact slotted patch resonator configurations operating 40 & 60GHz have ever been proposed. With the above reported development in the design of miniaturized patch resonators, it is now possible to realize compact duplexers using LTCC multilayer technology that cover two bands of interest for mobile communications such as broadband wireless local area networks (WLAN's) and local cellular radio network (LCRN). These dual-band duplexers can be designed around the 41/61GHz center frequencies (channel1/channel2) with <3dB insertion loss for both channels, and 6% 3-dB bandwidth below maximum insertion loss.

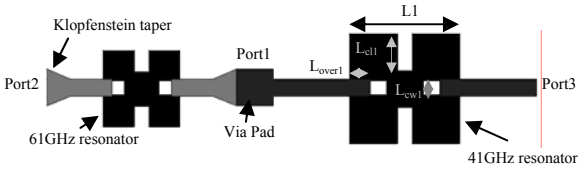

Fig. 7 Top view of the dual-band compact duplexer (41GHz/61GHz) consisting of two patch resonators connected together with a via junction

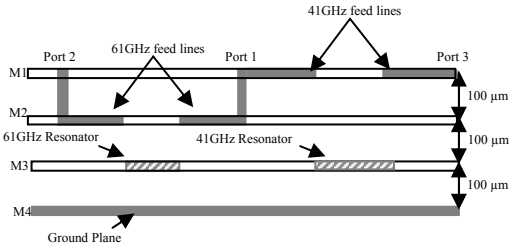

Fig. 8 Side view of the dual-band compact duplexer (41GHz/61GHz) in multilayer configuration.

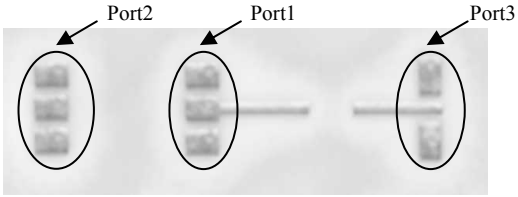

Fig. 9 Photograph of the duplexer fabricated in multilayer LTCC substrates (ε_r =5.4, tanδ=0.0015)

The top and side views of the topology chosen for the slotted patch duplexer are shown in figs. 7, 8, respectively. The two resonant patch filters are connected together with a via junction (Port1 in fig 7) which constitutes the common input. The 61GHz patch filter occupies the left portion of the diplexer and the 41GHz filter the right portion in fig 7. In comparison to the patch filter of Fig. 2b) that occupies four dielectric layers, the whole 41GHz patch filter is shifted up by one dielectric/metal layer so that it remains only three dielectric layers. This modification of the structure not only realizes a compact multilayer (3D) duplexer configuration, where the resonators are on the same metal layer while fed by strip lines on different layers (better isolation) but also makes it simpler to design by directly embedding the configuration designed in section A. In channel 1, this type provides a narrower bandwidth and a higher insertion loss since radiation from microstrip feedlines on the top (surface) layer is higher than from embedded types. The overlap (L_{over1} in fig7) works as main control-factor to improve the bandwidth as demonstrated in fig 5. The overlap (L_{over1}≈L/8.3) has been determined for a fixed dimension of the transverse cuts (L_{cw1}≈L/8.2, L_{cl1}≈L/3) with aid of IE3D. The slot length (L_{cl1} in fig7) is determined to fulfil target the insertion and center frequency specifications in the same way as the section A. In addition, the surface microstrip feedlines of channel 1 have been implemented in a way to achieve 50 Ω impedance matching and Klopfenstein impedance tapers have been employed to annihilate the parasitic coupling in microstrip discontinuities and to achieve impedance matching between the 61 GHz feedline and the via pad as shown in fig7. The fabricated duplexer (fig.9) occupies an

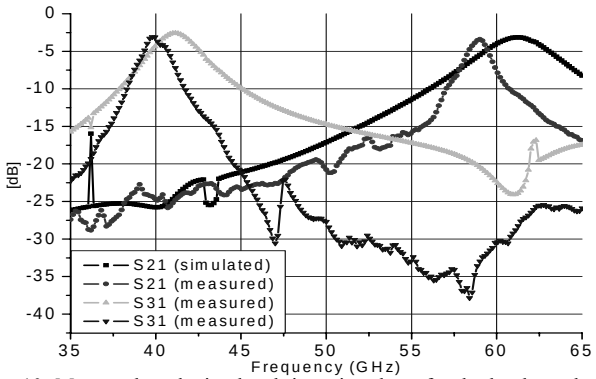

Fig. 10 Measured and simulated insertion loss for both channels of diplexer (Channel1:S31, Channel:S21)

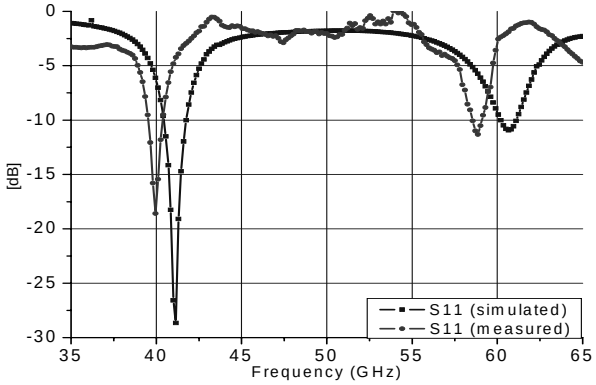

Fig. 11 Measured and simulated return loss (S11) for both channels of diplexer

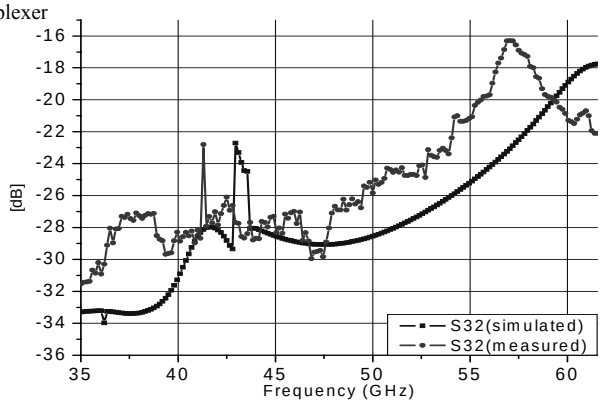

Fig. 12 Measured and simulated channel to channel isolation (S32).

area of 5.719 × 1.140 × 0.3 mm including the CPW measurement pads and the CPW-microstrip transition [18].

Figs. 10 and 11 show respectively the simulated and measured insertion and return losses of the duplexer. The measured insertion loss for channel 1 is 3.10 dB, which is slightly higher than the simulated value, while the return loss, shown in fig. 10, increases from -27 dB to -18.6 dB. The measured bandwidth is 4.8%, slightly smaller than the simulation results. Also, the center frequency is shifted to 39.8 GHz. For channel2, the measured insertion loss is 3.41dB slightly higher than the simulated value, while the return loss is -11.32 dB, a 6.68 dB decrease from the simulated value reported in fig 11. The measured bandwidth was about 3.25% which is quite smaller than the simulated values of 6%. The center frequency was also shifted to 59 GHz. The discrepancy between the simulated

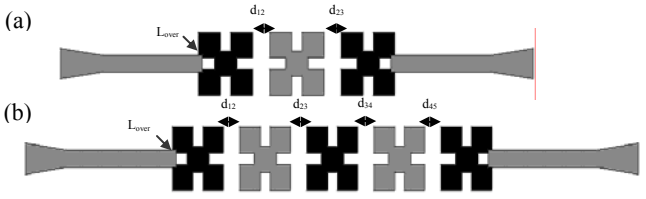

Fig. 13 The top view of (a) 3-pole slotted patch BPF (b) 5-pole slotted patch BPF

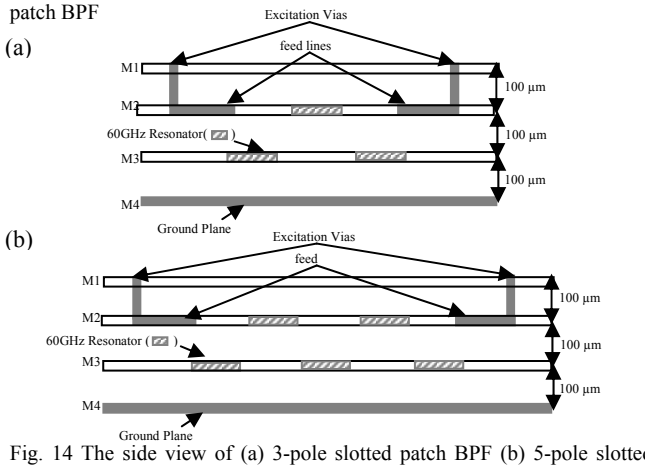

Fig. 14 The side view of (a) 3-pole slotted patch BPF (b) 5-pole slotted patch BPF

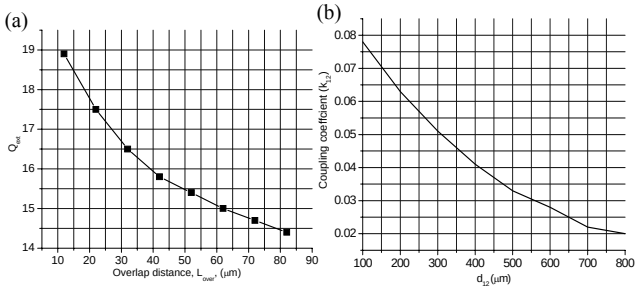

Fig 15. (a) External quality factor (Q_{ext}) evaluated as a function of overlap distance (L_{over}) (b) Coupling coefficient, k_{12}, as a function of coupling spacing (d_{12}) between 1st resonator and 2nd resonator.

and measured insertion/return loss values can be attributed to several factors: a) the fabrication accuracy of the feeding line /cut designs that have been computationally optimized for the original resonant frequencies and not for the shifted frequencies, and b) the additional conductor loss in measurements, due to the fact that the simulations assume that the metals of the strip feeding lines are perfect electric conductors. In addition, the narrower bandwidth in measurements compared to the simulations might be due to the fabrication accuracy of the vertical-coupling overlap design that is optimized for the original resonant frequencies and not for the shifted frequencies. The measured isolation agrees fairly well with the simulated values. Overall isolation is -29.5 dB at 39.8 GHz, -20.4 dB at 59 GHz and better than -16.3 dB in the worst case.

C. 3 AND 5 RESONATOR FILTER

We have designed and fabricated symmetrical three-pole and five-pole filters for inter-satellite wideband applications that consist of respectively three and five capacitively gap-coupled single-mode resonators, as shown figure 13 a) and b). The first 3-pole band pass filter was developed for a

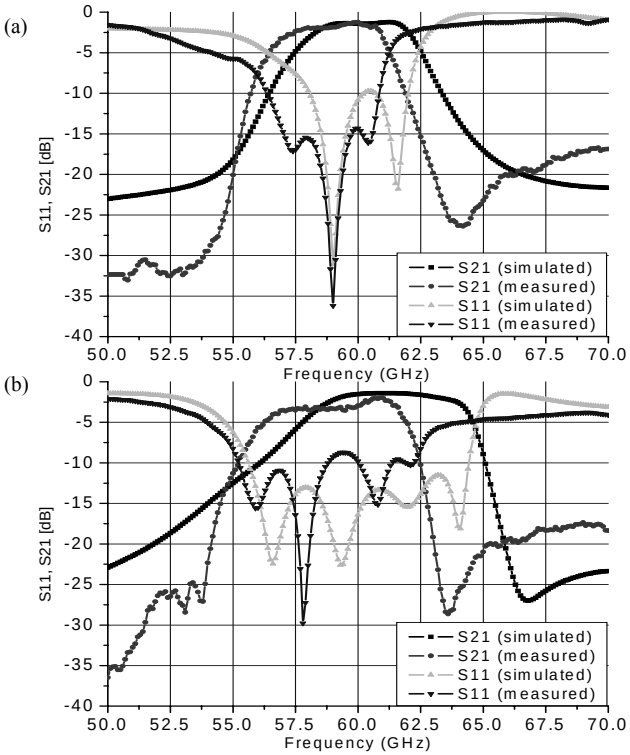

Fig. 16 Measured and simulated S-parameters of (a) 3-pole slotted patch BPF (b) 5-pole slotted patch BPF

center frequency of 59.6 GHz, 1dB insertion loss, 0.1 dB in band ripple and 6.4% fractional bandwidth based on Chebyshev lowpass prototype filter. The design parameters such as the external quality factors and the coupling coefficients, were decided to be

$$Q_{ext} = 15.4725$$
$$k_{12}=k_{23} = 0.06128$$

To determine the physical dimensions, full-wave EM simulations (IE3D) were used to extract the coupling coefficients ($k_{ii+1,\ i=1or2}$) and external quality factors (Q_{ext}) based on a simple graphical approach as described in [6]. Feeding lines and slotted patch resonators were alternatively located on different metal layers (feeding lines, 2nd resonator: M2; 1st resonator, 3rd resonator :M3) as shown in fig. 14 a) to achieve strong k_{ii+1} between resonators as well as desired Q_{ext} between resonator and feeding line with a moderate sensitivity to the LTCC fabrication tolerances. Fig 15 a) shows the Q_{ext} evaluated as a function of overlap distance (L_{over}). A larger L_{over} results in a stronger input/output coupling and smaller Q_{ext}. Then the required k_{ij} is obtained against the variation of distance (d_{ij} in fig. 13 a)) for a fixed Q_{ext} at input/output ports. Full-wave simulation was also employed to find two characteristic frequencies (f_{p1}, f_{p2}) that represent resonant frequencies of coupled structure when an electrical wall or a magnetic wall, respectively, was inserted in the symmetrical plane of coupled structure [11]. Characteristic frequencies were associated to the coupling between resonators as following: $k = (f_{p2}^2 - f_{p1}^2)/(f_{p2}^2 + f_{p1}^2)$ [11]. The coupling spacing (d_{12} in fig. 13 a) between the first and second resonators for the required k_{12} was determined from

fig 15 b). k_{23} and d_{23} are determined the same way as k_{12} and d_{12} since the investigated filter is symmetrical around its center.

Fig 16 a) shows the comparison of the simulated and the measured S-parameters of the 3-pole slotted patch filter. Good correlation is observed and the filter exhibits an insertion loss < 1.235 dB, the return loss >14.311 dB over pass band, and the 3dB bandwidth about 6.6 % at center frequency 59.1GHz. The selectivity on high side of the passband is better than EM simulation because an inherent attenuation pole occurs at the upper side. The latter is due to the fact that the space between fabricated nonadjacent resonators might be smaller than that in simulation so that stronger cross coupling might occur. In addition, the measured insertion loss is slightly higher than the theoretical result because of additional conductor loss and radiation loss from the feeding microstrip lines that can not be de-embedded because of the nature of SOLT. The dimension of the fabricated filter is 5.855 mm × 1.140 mm × 0.3 mm with measurement pads.

A high-order filter design using 5 slotted patches (fig. 13 b)) and having very similar coupling scheme than the 3 pole filter was investigated. The Chebyshev prototype filter was designed for a center frequency of 61.5 GHz, 1.3 dB insertion loss, 0.1 dB band ripple and 8.13% 3-dB bandwidth. The circuit parameters for this filter are:

$$Q_{ext} = 14.106$$
$$k_{12}=k_{45} = 0.0648$$
$$k_{23}=k_{34} = 0.0494$$

Fig. 14 b) shows the side view of 5-pole slotted patch BPF. The feeding lines and the open-circuit resonators have been inserted into the different metallization layers (feeding lines, 2nd resonator, 4th resonator: M2; 1st resonator, 3rd resonator, 5th resonator: M3) so that the spacing between adjacent resonators and the overlap between the feeding lines and the resonators work as the main parameters of the filter design to achieve the desired coupling coefficients and the external quality factor. The same technique is applied to the design of 3 poles BPF. The filter layout parameters are: $d_{12}=d_{45}\approx\lambda_{go}/16$, $d_{23}=d_{34}\approx\lambda_{go}/11$, $L_{over}\approx\lambda_{go}/26$ (fig. 13 b)) where λ_{go} is the guided wavelength and the filter size is 7.925×1.140×0.3mm3. The measured insertion and reflection loss of the fabricated filter are compared with the simulated results in fig. 16 b). The fabricated filter exhibits a center frequency of 59.15 GHz, an insertion loss of about 1.386 dB, and a 3-dB bandwidth of approximately 7.98%. These multi-pole filters can be used in the development of a multi-pole duplexer.

III. 40GHz Directional Filter

This paragraph presents one 40 GHz 4-ports directional filter with excellent performance in LTCC technology. As shown, in fig 16, the device exhibits a band-rejection characteristic between ports 1 and 2, and a band-pass characteristic between ports 1 and 4. The other port (#3) is isolated from the input (port1) [12]. The integrated structure is symmetric. This multifunctional device can be

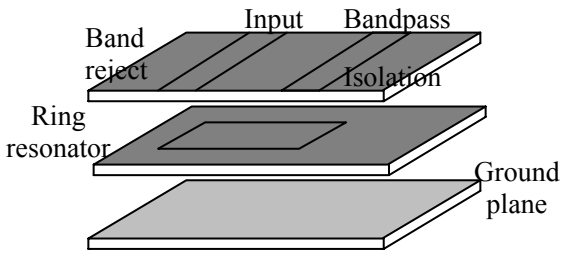

Fig. 17 Implementation of the directional filter in multilayer LTCC substrate

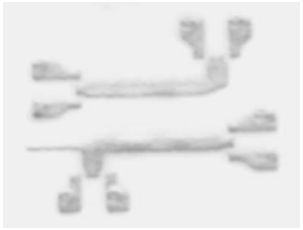

Fig.18 Photo of fabricated directional filters

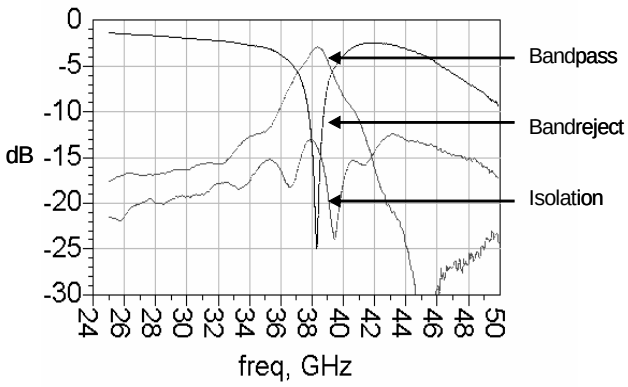

Fig.19 Performance of the directional filter

applied for mm-wave passive mixers to mix RF and LO signals with IF signal with required isolation. Sharp frequency selective nature of the directional filters can also be utilized in the design of mm-wave multiplexers and demultiplexers. Simple and compact implementation has been achieved using embedded microstrip lines with a reduced number of metal layers as compared to a stripline topology. The high quality factor of the ring resonator assures the narrowband operation and, hence, this topology can be used efficiently in frequency selective applications.

In this single loop directional filter, the coupling between the transmission lines has been achieved by vertically coupled structures alleviating the need of a very narrow broadside (horizontal) coupling distance, which could not be realized in LTCC. The effective lengths of all sides of the ring have been made equal to one quarter of the guided wavelength. The feeding top layer transmission line has been designed to be 50ohm microstrip line. The width of the coupled section of the ring has been chosen so that there is minimum reflection in the frequency of interest in the coupled section of ring. The uncoupled sections of the ring are 50ohm embedded microstrip lines so that the ring provides minimum mismatch at the frequency of interest. At the frequency band of operation, the signal couples from

the input transmission line to the embedded ring and hence the required band-pass and band-reject characteristics are achieved (fig 17). The dielectric thickness is 100um between the metal layers and it occupies an area of 2mm×2mm.

The layout and the performance of the filter are shown in figs.18, 19 respectively. The band-pass section shows a measured insertion loss of <3 dB and the band-reject section exhibits a rejection of ~25 dB at around 38.5 GHz. This is the first reported mm-wave directional filter fabricated in LTCC process. Traditionally designers have designed waveguide directional filter or traveling wave directional filters [19] introduces the design of microstrip loop directional filters at a much lower frequency (10GHz). A. P. Gorbachev [20] shows a wideband performance at a much lower RF frequency. In this work, we present simple, compact, low-cost microstrip design with excellent narrowband frequency selectivity at mm-wave.

IV. Cross-Shaped Microstrip Antenna

A cross-shaped antenna has been designed for the transmission and reception of signals that cover two bands between 59-64 GHz. The first band (channel 1) covers 59-61.25 GHz, while the second band (channel 2) covers 61.75-64 GHz. This antenna can be easily integrated within a wireless millimeter-wave module containing the components of the previous section. Its structure is dual-polarized for the purpose of doubling the data output rate transmitted and received by the antenna. The cross-shaped geometry was utilized to decrease the cross-polarization which contributes to unwanted sidelobes in the radiation pattern [13].

The antenna, shown in Fig.20, was excited by proximity-coupling and had a total thickness of 12 metal layers and 11 substrate layers (each layer was 100 μm thick). Proximity-coupling is a particular method for feeding patch antennas where the feedline is placed on a layer between the antenna and the ground plane. When the feedline is excited, the fringing fields at the end of the line strongly couple to the patch by electromagnetic coupling. This configuration is a non-contact, non-coplanar method of feeding a patch antenna. The use of proximity-coupling allows for different polarization reception of signals that exhibits improved cross-channel isolation in comparison to a traditional coplanar microstrip feed. There were two substrate layers separating the patch and the feedline, and two substrate layers separating the feedline and the ground layer. The remaining seven substrate layers are used for burying RF circuitry beneath the antenna that includes the filter, integrated passives and other components. The size of the structure was 8×7mm2. A right angle bend in the feedline of channel 2 is present for the purpose of simplifying the scattering parameter measurements on the network analyzer.

The design was simulated using the TLM-based, 3D full-wave solver MicroStripes 6.0. Fig. 21 a) shows the

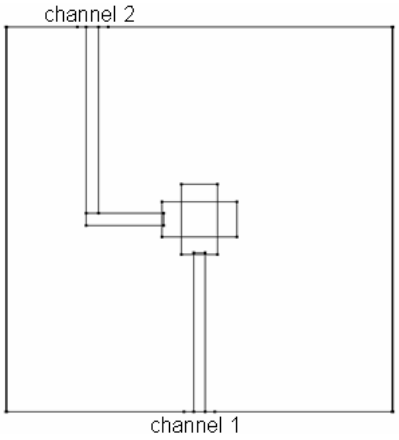

Fig. 20 Antenna Structure

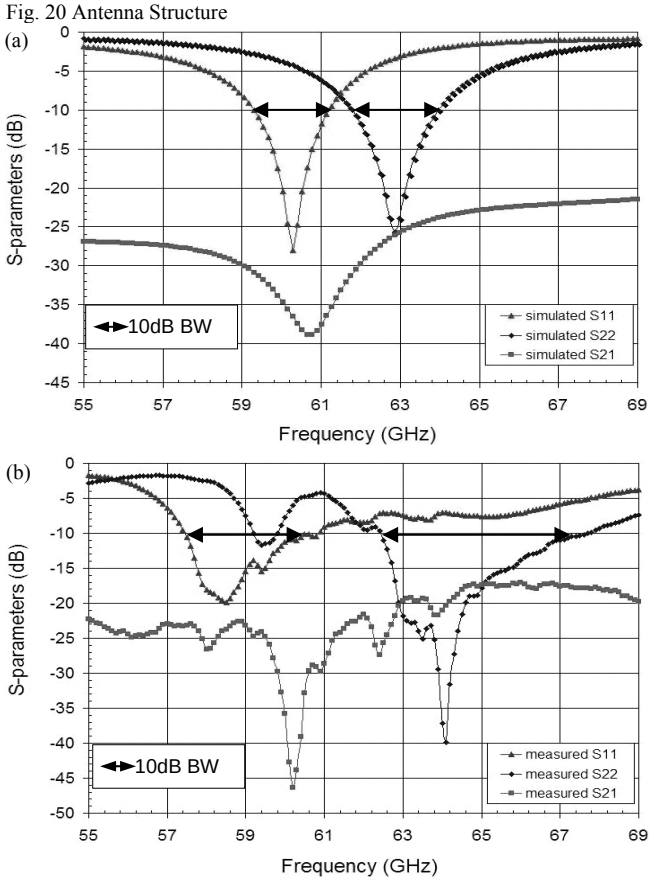

Fig. 21 (a) Simulated and (b) measured S-Parameter data versus frequency Antenna Structure

simulated scattering parameters versus frequency for this design. The targeted frequency of operation was around 60.13 GHz for channel 1 (S11) and 62.87 GHz for channel 2 (S22). The simulated return loss for channel 1 was close to -28dB at f_r = 60.28 GHz, while for channel 2, the return loss was ~ -26dB at f_r = 62.86 GHz. The simulated frequency for channel 1 was optimized in order to cover the desired band based on the antenna structure. Channel 2 has a slightly greater bandwidth (3.49%) than that of channel 1 (3.15%) primarily due to the right angle bend in the feedline that can cause small reflections to occur at neighboring frequencies near resonance point of the lower band. The upper edge frequency (f_H) of the lower band is

61.21 GHz; while the lower edge frequency (f_L) of the higher band is 61.77 GHz. Fig. 21 b) shows the measured scattering parameters versus frequency for the design. The measured return loss for channel 1 (-20dB @ f_r = 58.5 GHz) is worse than that obtained through the simulation (-26dB). Conversely, the -40dB of measured return loss at f_r = 64.1 GHz obtained for channel 2 is significantly better than the simulated return loss of -28dB. The diminished return loss of channel 1 is acceptable due to minor lossesassociated with measurement equipment (cables, connectors, etc…). The enhanced return loss of channel 2 could result from measurement inaccuracies or constructive interference of parasitic resonances at or around the TM_{10} resonance. The asymmetry in the feeding structure may account for this difference in the measured return loss. Frequency shifts for both channels are present in the measured return loss plots. Additionally, the bandwidths of the two channels are wider than those seen in simulations (5.64% for channel 1 and 8.26% for channel 2). Small deviations in the dimensions of the fabricated design as well as measurement tolerances may have contributed to the frequency shifts, while the increased bandwidths may be attributed to radiation from the feedlines and other parasitic effects that resonate close to the TM_{10} mode producing an overall wider bandwidth. The upper edge frequency (f_H) of the lower band is 61 GHz, while the lower edge frequency (f_L) of the higher band is 62.3 GHz. The simulated cross-coupling between channels 1 and 2 (Fig. 20) is below -22 dB for the required bands. On the other hand, the measured cross-coupling between the channels is below -22dB for the lower band and below -17dB for the upper band. Due to the close proximity of the feeding line terminations of the channels, the cross-coupling is hindered, but these values are satisfactory for this application.

V. CONCLUSION

The development of various advanced 3-D LTCC system-on-package passives solutions for compact, low-cost wireless front-ends to be used in millimeter-wave frequency ranges has been presented. A new class of compact and easy-to-design passive functions, such as filters, directional filters and antennas, have been demonstrated with excellent performance and high integration potential. The patch resonator filter that uses vertical coupling overlap and transverse cuts as design parameters achieves a high level of miniaturization and a great compromise between size and power handling. The excellent performance of the patch resonator filter is verified through a measured insertion loss better than 2.3 dB and a return loss larger than 18.2 dB over the pass-band, and a bandwidth of about 6.4%. On the basis of the single-mode patch resonator, a multilayer compact diplexer and multistage (3pole & 5pole) bandpass filters have been fully characterized and have demonstrated performances suitable for V-band mobile communication and inter-satellite wideband applications. Directional filters have been experimentally verified to provide easy and compact solutions for applications, such as mixing and multiplexing with a measured insertion loss better than 3dB over the band-pass section and a rejection of ~ 25dB at around 38.5GHz over the band rejection section. A double fed cross-shaped microstrip antenna has been designed for the purpose of effectively doubling the data through-put by means of dual polarized wireless channel, covering the band between 59-64 GHz. This antenna can be easily integrated into a wireless millimeter-wave module along with the other RF components.

ACKNOWLEDGEMENT

The authors wish to acknowledge the support of the Georgia Tech., Packaging Research Center, the Georgia Electronic Design Center, the NSF Career Award #ECS-9984761, and the NSF Grant #ECS-0313951.

REFERENCES

[1] K.Lim, S.Pinel, M.F.Davis, A.Sutono, C.-H.Lee, D.Heo, A.Obatoynbo, J.Laskar, E.M.Tentzeris, and R.Tummala, "RF-System-On-Package (SOP) for Wireless Communications," *IEEE Microwave Magazine*, Vol.3, No.1, pp.88-99, Mar. 2002.

[2] J.Lee, K.Lim, S.Pinel, G.DeJean, R.L.Li, C.-H.Lee, M.F.Davis, M.Tentzeris, and J.Laskar, "Advanced System-on-Package (SOP) Multilayer Architectures for RF/Wireless Systems up to Millimeter-Wave Frequency Bands," in *Proc. Asian Pacific Microwave Conference*, Seoul, Korea, Nov. 2003, pp. FA5_01.

[3] V.Kondratyev, M.Lahti, and T.Jaakola, "On the design of LTCC filter for millimeter-waves," in *2003 IEEE MTT-S Int. Microwave Sym. Dig.*, Philadelphia, PA., June 2003, pp. 1771-1773.

[4] R.L.Li, G.DeJean, M.M.Tentzeris, J.Laskar, and J.papapolymerou, "LTCC Multilayer based CP Patch Antenna Surrounded by a Soft-and-Hard Surface for GPS Applications," in *2003 IEEE-APS Symposium*, Columbus, OH, June 2003, pp.II.651-654.

[5] C.H.Lee, A.Sutono, S.Han, K.Lim, S.Pinel, J.Laskar, and E.M.Tentzeris, "A Compact LTCC-based Ku-band Transmitter Module," *IEEE Transactions on Advanced Packaging*, Vol.25, No.3, , Aug. 2002, pp.374-384.

[6] Y.Rong, K.A.Zaki, M.Hageman, D.Stevens, and J.Gipprich, "Low-Temperature Cofired Ceramic (LTCC) Ridge Waveguide Bandpass Chip Filters," *IEEE Transaction on Microwave Theory and Technique*, Vol. 47, No. 12, pp. 2317-2324, Dec. 1999.

[7] Yong Huang, "A Broad-Band LTCC Integrated Transition of Laminated Waveguide to Air-Filled Waveguide for Millimeter-Wave Applications," *IEEE Transaction on Microwave Theory and Technique*, Vol. 51, No. 5, pp. 1613-1617, May 2003.

[8] W.-Y.Leung, K.-K.M.Cheng, and K.-L.Wu, "Multilayer LTCC Bandpass Filter Design with Enhanced Stopband Characteristics," *IEEE Microwave and Wireless Components Letters,* Vol.12, No. 7, pp. 240-242, May 2002.

[9] Y. Rong, K.A.Zaki, M.Hageman, D.Stevens, and J.Gipprich, "Low Temperature Cofired Ceramic (LTCC) Ridge Waveguide Multiplexers," in *2000 IEEE MTT-S Int. Microwave Sym. Dig.,* Boston, MA., June 2000, pp. 1169-1172.

[10] R.Lucero, W.Qutteneh, A.Pavio, D.Meyers, and J.Estes, "Design of An LTCC Switch Diplexer Front-End Module for GSM/DCS/PCS Application," in *2001 IEEE Radio Frequency Integrated Circuit Sym.,* Phoenix, AZ., May 2001, pp. 213-216.

[11] J.-S.Hong and M.J.Lancaster, "Coupling of microstrip square open-loop resonators for cross-coupled planar microwave filters," *IEEE Transaction on Microwave Theory and Technique*, Vol. 44, No. 12, pp. 2099-2109, Dec. 1996.

[12] G.L.Matthaei, L.Young, and E.M.T.Jones, *Microwave filters, impedance-matching networks, and coupling structures*, Nort Bergen, NJ/U.S.A.: Bookmart Press, 1985.

[13] A.Tavakoli, N.Darmvandi, and R.M.Mazandaran, "Analysis of cross-shaped dual-polarized microstrip patch antennas," in *1995 IEEE AP-S Int. Sym. Dig.*, Newport Beach, CA., June 1995, pp. 994 – 997.

[14] J.-H.Lee, G.DeJean, S.Sarkar, S.Pinel, K.Lim, J.Papapolymerou, J.Laskar, and M.M.Tentzeris, "Advanced 3-D LTCC system-on-package (SOP) architectures for highly integrated millimetre-wave wireless systems," presented at *Proc. 34th European Microwave Conference*, Amsterdam, Nederland, 2004.
[15] H.H.Meinel, "Commercial Applications of Millimeterwaves History, Present Status, and Future Trends," *IEEE Transaction on Microwave Theory and Technique*, Vol. 43, NO. 7, pp. 1639-1653, July 1995.
[16] D.M.Pozar and D.H.Schaubert , *Microstrip Antennas*, New York, NY/ U.S.A: IEEE press, 1995.
[17] Robert E. Collin, *Foundations for Microwave Engineering*, New York, NY/U.S.A: McGraw Hill, 1992.
[18] Wojciech Wiatr, "Coplanar-Waveguide-to-Microstrip Transition Model," in *2000 IEEE MTT-S Int. Microwave Sym. Dig*, Boston, MA., June 2000, pp. 1797-1800.
[19] S Uysal, "Microstrip Loop Directional Filter," *Electronics Letters*, Vol. 33, No. 6, pp. 475-476, March 1997.
[20] A P Gorbachev. "The Reentrant Wide-Band Directional Filter," *IEEE Transactions on Microwave Theory and Techniques* Vol.50, No.8, pp. 2028-2031, Aug. 2002.
[21] D.M.Pozar and D.H.Schauber, Microstrip Antennas, Piscataway, NJ/U.S.A.:IEEE press, 1995.